SLAC-PUB-9471
August 2002

Combined phenomena of beam-beam and beam-electron cloud effects in circular e^+e^- colliders

K. Ohmi, [2] A. W. Chao
KEK, Oho, Tsukuba, 305-0801, Japan
[2] *SLAC, Stanford, CA94309, USA*

Abstract

An electron cloud causes various effects in high intensity positron storage rings. Positron beam and electron cloud can be considered a typical two stream system with a plasma frequency. Beam-beam effect is also an important issue for high luminosity circular colliders. Colliding two beams are considered as a two-stream system with another plasma frequency. We study combined phenomena of the beam-electron cloud and beam-beam effects from a viewpoint of two complex "two stream effects" with two plasma frequencies.

1 INTRODUCTION

In recent high intensity positron rings, various phenomena related to electron cloud have been observed. Coupled bunch instabilities have been observed at KEK Photon Factory and IHEP-BEPC, and beam size enlargements have been observed at B factories of SLAC (PEP-II) and KEK (KEKB). These phenomena were understood as two-stream instability of relativistic beam and slow electron cloud. The phenomena can also be understood as instabilities which is caused by wake force due to electron cloud. The coupled bunch instability is the two-stream effect characterized by average plasma frequency along bunch train, or is mediated by long range wake force of the order of bunch spacing ($\sim$1m). The beam size enlargement is the two-stream effect characterized by plasma frequency in a bunch, or mediated by short range wake force of the order of bunch length ($\sim$1cm). The positron beam, which is perturbed by the electron cloud, interacts with an electron beam in a collider. The colliding beams are regarded as a two-stream system with a plasma frequency characterized by the beam-beam force. The beam-beam interaction has a nature of a short range wake force, namely, a distortion of head part of a beam, which induces a perturbation of another beam, affects the tail part of itself. The short range wake force due to electron cloud and the beam-beam force may couple each other and cause a kind of combined phenomena.

Such combined phenomana may have been observed in KEKB. The transverse size of positron beam is enlarged beyond a threshold current due to the short range wake force at an operation with only positron beam. Luminosity is extremely low for bunch spacing narrower than 6ns even below the threshold current of the beam enlargement [1].

We study combined phenomena of the two types of "two stream system". We first discuss this instability using linearized one-two-particle model, in which e^- and e^+ beams are represented by one and two-particles, respectively. The beam-beam force is linearized in the model. The wake force due to electron cloud is approximated to be a constant along the longitudinal direction. Similar system has been studied in Refs. [2] for ordinary wake force. The combined effects based on the weak-strong beam-beam model have been discussed in Ref.[3].

We next discuss the phenomena using a tracking simulation in which each of the two beam is represented by a large number ($\sim$1,000) of macro-particles (or slices) distributed in the longitudinal phase space[4]. Each macro-particle has a transverse beam size determined by the emittance and the beta function, and nonlinearity for their interaction are taken into account. Electron cloud is represented by many ($\sim$10,000) point-like macro-particles. The beam-electron cloud interaction is evaluated by interaction between transverse Gaussian beam and each macro-electron[4].

2 TWO-STREAM FEATURES OF BEAM-ELECTRON CLOUD AND BEAM-BEAM SYSTEMS

We discuss linear theory of the combined system of beam-beam and wake field. Similar system has been already studied by E. A. Perevedentev and A. A. Valishev [2]. We study the system using an alternative point of view: *i.e.*, combined effect of beam-beam and beam-electron cloud. We start discussions of beam-electron cloud interaction. The beam-electron cloud system is a typical model of the two-stream instability. The beam slices and the cloud electrons obey the equation of motion as follows,

$$\frac{d^2\boldsymbol{x}_{e,a}}{dt^2} = -2\lambda_+(s_+)r_e c\boldsymbol{F}_G(\boldsymbol{x}_{e,a}-\bar{\boldsymbol{x}}_{+,j};\boldsymbol{\sigma})\delta(t-t_j(s_e)), \tag{1}$$

$$\frac{d^2\boldsymbol{x}_{+,j}}{ds^2}+\left(\frac{\omega_\beta}{c}\right)^2 = -\frac{2r_e}{\gamma}\sum_{a=1}^{N_e}\boldsymbol{F}_G(\bar{\boldsymbol{x}}_{+,j}-\boldsymbol{x}_{e,a};\boldsymbol{\sigma})\delta(s-s_e). \tag{2}$$

where the force $\boldsymbol{F}_G(\boldsymbol{x})$ is expressed by the Bassetti-Erskine formula normalized so that $\boldsymbol{F}_G \rightarrow \boldsymbol{x}/|\boldsymbol{x}|^2$ as $\boldsymbol{x}\rightarrow\infty$.

Electrons oscillate with an angular frequency due to the linear part of $\boldsymbol{F}_G$,

$$\omega_{e,y(x)} = \sqrt{\frac{\lambda_+ r_e}{(\sigma_{+,x}+\sigma_{+,y})\sigma_{+,y(x)}}}, \tag{3}$$

Work supported by the Department of Energy contract DE-AC03-76SF00515.

where λ_+ and $\sigma_{+,x(y)}$ are line density and horizontal (vertical) size, respectively, of the positron beam. $\omega_{e,y}$ and $\omega_{e,x}$ are about $1.9 \times 10^{11} s^{-1}$ and $7.2 \times 10^{10} s^{-1}$, respectively, with the KEKB parameters: *i.e.*, $\sigma_x = 420 \mu m$, $\sigma_y = 60 \mu m$, $\sigma_z = 5mm$ and $N_+ = 3.3 \times 10^{10} m^{-1}$. ω_e is considered as plasma frequency for the two-stream system of the beam-electron cloud. The phase advance of the electron motion during the interaction, $\phi_e = \omega_e \sigma_z / c$, characterizes the instablity. For KEKB, $\phi_{e,y} = \omega_{e,y} \sigma_z / c \approx 2.5$ and $\phi_{e,x} = \omega_{e,x} \sigma_z / c \approx 1.0$.

The beam-beam system also has a potential to cause a two-stream instability, because one beam oscillates in electro-magnetic field produced by the other beam with a certain frequency. The beam-beam force is expressed in linear regime as follows,

$$\frac{d^2 \boldsymbol{x}_{\pm,j}}{ds^2} + \left(\frac{\omega_\beta}{c}\right)^2 = -\frac{2r_e}{\gamma} \sum_{a=1}^{N_\mp} \boldsymbol{F}_G(\bar{\boldsymbol{x}}_{\pm,j} - \boldsymbol{x}_{\mp,a}; \boldsymbol{\Sigma}) \delta(s - s_\mp). \tag{4}$$

where $\Sigma_{x(y)} = \sqrt{\sigma^2_{+,x(y)} + \sigma^2_{-,x(y)}}$. Each of the beam slices is assumed to be rigid Gaussian with rms beam size $\sigma_{\pm,x(y)}$.

There is a coherent frequency during the interaction between the two beams given as follows,

$$\omega_{\pm,y(x)} = \sqrt{\frac{\lambda_\mp r_e}{\gamma_\pm (\sigma^*_{\mp,x} + \sigma^*_{\mp,y}) \sigma^*_{\mp,y(x)}}} \tag{5}$$

where $\gamma_\pm$ is the relativistic factor of positron and/or electron beam. We note that $\sigma^*_{\pm,x(y)}$, the beam size of positron and/or electron beam at an interaction point, is much smaller than $\sigma_{x(y)}$ in Eq.(3), and $\gamma \gg 1$.

The phase advance, ϕ, of the oscillation during a collision is expressed by

$$\phi_{\pm,y(x)} = \frac{\omega_{\pm,y(x)} \sigma_z}{c} = \sqrt{\frac{2\pi \xi_{y(x)} \sigma_z}{\beta_{y(x)}}} \equiv \sqrt{D_{y(x)}}, \tag{6}$$

where ξ_y is the beam-beam parameter and we have assumed that two beams have the same beam size. We call $D \equiv \phi^2_\pm$ the beam-beam disruption parameter. ϕ_y is approximately the order of unity for recent high luminosity colliders. The two-stream effect may be important under this condition. $\phi_x = \sqrt{\xi_x \beta_y / \xi_y \beta_x} \phi_y$ is smaller than ϕ_y, but the horizontal effect may be important depending on the tune as will be shown later.

3 ONE-TWO-PARTICLE MODEL

We first study the phenomena using a small number of macro-particles; i.e. one-two-particle model. The electron and positron beams are represented by one and two macro-particles, respectively, in the model. The model is reliable approximation for considering the beam-beam interaction, since the phase advance, $\phi_\pm$, is less than 1 in most cases. Furthermore the beam-electron cloud interaction is approximated to be described by a constant wake force. Although ϕ_e is larger than 1, and therefore the model is beeing stretched, we believe that the analysis remains reasonable. An analytic treatment becomes possible by the approximation.

We discuss vertical motion below. Motion of the two beams is characterized by a vector $\boldsymbol{Y}(s)$.

$$\boldsymbol{Y}(s) = (y_1^+, p_1^+, y_2^+, p_2^+, y^-, p^-)^t, \tag{7}$$

where the suffix t denotes the transpose of the matrix or vector. We consider a revolution matrix to transfer $\boldsymbol{Y}(s^* + C)$ from $\boldsymbol{Y}(s^*)$, where s^* and C are position of interaction point and circumference of a ring, respectively. The beam size (beta function) is temporarily assumed to be a constant during the collision. The synchrotron tune is assumed to be inverse of an integer ($\nu_s = 1/n_s$). We try to study for general synchrotron tune later. In particular, the tracking simulation discussed later is not limited to particular values of the synchrotron tune. The beam-beam force does not have a longitudinal component, since beta function is assumed to be constant. The two particles in the positron beam have an opposite synchrotron phase. The macro-electron always stays at the center of mass. The collision points of the two macro-positrons and the macro-electron are given by $s^* + \Delta$, where

$$\Delta = \pm \frac{\sigma_z}{2} \sin(2\pi \nu_s s / C). \tag{8}$$

The collision of i-th positron and the electron is represented by a matrix $B_i(\xi)$

$$B_1(\xi) = \begin{pmatrix} I + b(2\xi) & 0 & -b(2\xi) \\ 0 & I & 0 \\ -b(\xi) & 0 & I + b(\xi) \end{pmatrix}. \tag{9}$$

$$B_2(\xi) = \begin{pmatrix} I & 0 & 0 \\ 0 & I + b(2\xi) & -b(2\xi) \\ 0 & -b(\xi) & I + b(\xi) \end{pmatrix}. \tag{10}$$

where

$$b(\xi) = \begin{pmatrix} 0 & 0 \\ -\pi\xi & 0 \end{pmatrix}, \tag{11}$$

and I is 2×2 unit matrix.

Transfer matrix of collision at $s = \Delta$ is expressed by $B(\Delta) = D^{-1}(\Delta) B D(\Delta)$: that is, particles drift to $s = \pm\Delta$, collide and return to the interaction point. The matrix $D(\Delta)$ is expressed by

$$D(\Delta) = \begin{pmatrix} d(\Delta) & 0 & 0 \\ 0 & d(\Delta) & 0 \\ 0 & 0 & d(-\Delta) \end{pmatrix}, \tag{12}$$

where

$$d(\Delta) = \begin{pmatrix} 1 & \Delta \\ 0 & 0 \end{pmatrix}. \tag{13}$$

The transfer matrix of the collision is expressed by

$$\boldsymbol{Y}_{after}(s^*) = T_{BB}(\Delta) \boldsymbol{Y}_{before}(s^*), \tag{14}$$

where T_{BB} has two ways of representations depending on the sign of Δ: *i.e.*, which particle is at the bunch head or tail. When the first particle stays at the head of the bunch ($\Delta > 0$) in a half synchrotron period, the matrix is expressed by

$$T_{BB}(\Delta) = D^{-1}(-\Delta)B_2 D(-\Delta)D(\Delta)^{-1}B_1 D(\Delta) \tag{15}$$

In the other half synchrotron period ($\Delta < 0$), it is expressed by

$$T_{BB}(\Delta) = D^{-1}(\Delta)B_1 D(\Delta)D^{-1}(-\Delta)B_2 D(-\Delta). \tag{16}$$

The particles are transferred along arc section after the collision ($s = s^*$) to the collision point ($s = s^* + C$). The wake field affects the tail particle depending on betaton amplitude of the head particle. The transfer matrix from s^* to $s^* + C$ has two representations depending on the sign of Δ again. The matrix (T_{arc}) for $\Delta > 0$ is expressed by

$$T_{arc} = \begin{pmatrix} T_2(\mu_1) & 0 & 0 \\ A(W,\mu_1) & T_2(\mu_2) & 0 \\ 0 & 0 & T_2(\mu_e) \end{pmatrix}, \tag{17}$$

For $\Delta < 0$,

$$T_{arc} = \begin{pmatrix} T_2(\mu_1) & A(W,\mu_2) & 0 \\ 0 & T_2(\mu_2) & 0 \\ 0 & 0 & T_2(\mu_e) \end{pmatrix}, \tag{18}$$

where

$$T_2(\mu) = \begin{pmatrix} \cos\mu & \sin\mu \\ -\sin\mu & \cos\mu \end{pmatrix}. \tag{19}$$

$\mu_i = 2\pi\nu_i$ is betatron phase advance including chromatic modulation.

$$\mu_1 = \mu_p + \mu_s\chi\sin\frac{\omega_s}{c}s, \quad \mu_2 = \mu_p - \mu_s\chi\sin\frac{\omega_s}{c}s, \tag{20}$$

where

$$\chi = \frac{2\pi Q'}{\alpha L} = \frac{Q'\sigma_\delta}{\nu_s}. \tag{21}$$

$A(W,\mu)$, which describes the kick caused by the wake field is expressed by

$$A(W,\mu) = \begin{pmatrix} (W/2)\sin\mu & -(W/2)\cos\mu \\ (W/2)\cos\mu & (W/2)\sin\mu \end{pmatrix}. \tag{22}$$

The revolution matrix including the transfer of the arc section and the beam-beam interaction is expressed by

$$T_{rev}(\Delta) = T_{BB}(\Delta)T_{arc}(W,\mu), \tag{23}$$

where Δ is given by Eq.(8).

We calculate the transfer matrix for one synchrotron period ($\nu_s = 1/n_s$),

$$T_{syn} = \prod_{i=1}^{n_s} T_{rev}(\Delta_i). \tag{24}$$

The stability of the system can be discussed by eigenvalues of the 6×6 matrix (T_{syn}). The matrix is not symplectic, but its determinant is unity, because of $A(W)$. The eigenvalues are calculated numerically. When an imaginary part of the eigenvalues is nonzero, the system becomes unstable.

We first discuss vertical motion. Figure 1 shows the imaginary part of the eigenvalues as functions of betatron tune. For $W = 0$, nonzero values of imaginary part occurs only near the half integer tune as is shown in the upper picture. For $W > 0$, nonzero imaginary part occurs for all tunes: *i.e.*, the system always unstable regardless of the tune.

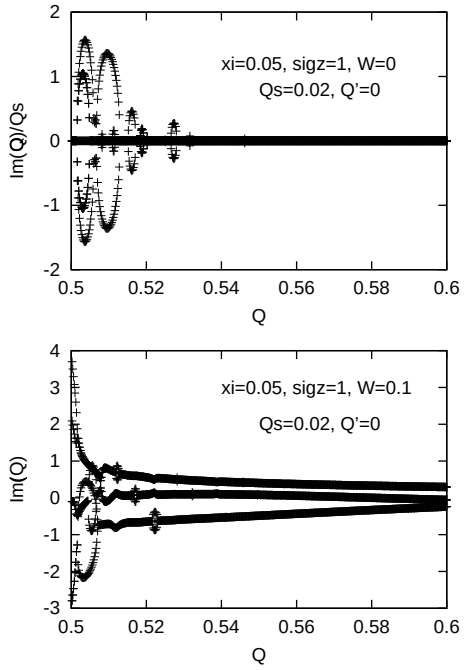

Figure 1: Variation of imaginary part of the eigenvalues depending on the betatron tune. Beam-beam parameter is chosen to be 0.05. Upper and lower pictures are for W=0 and W=0.1, respectively.

Figure 2 shows the imaginary parts as functions of the strength of the wake field and beam-beam parameter. The behavior for the wake strength is simple but that for the beam-beam parameter is complex. The beam-beam kicks depend on the longitudinal coordinate. The complex beam-beam behavior may be similar to the behavior of chromaticity for head-tail effect. Figure 3 shows the chromaticity dependence of the imaginary part of the eigenvalues.

We now discuss horizontal effect. The phase advance of beam-beam disruption is less than vertical one, because $\phi_x \approx \sqrt{\beta_y/\beta_x}\phi_y$ in ordinary colliders ($\xi_x \approx \xi_y$), while $\beta_y \ll \beta_x$. However we use an operating point slightly above a half integer horizontal tune in KEKB to get a benefit from dynamical beta effect. Horizontal effect may be therefore important though ϕ_x is small. Figure 4 shows the imaginary part of the eigenvalus of the horizontal matrix.

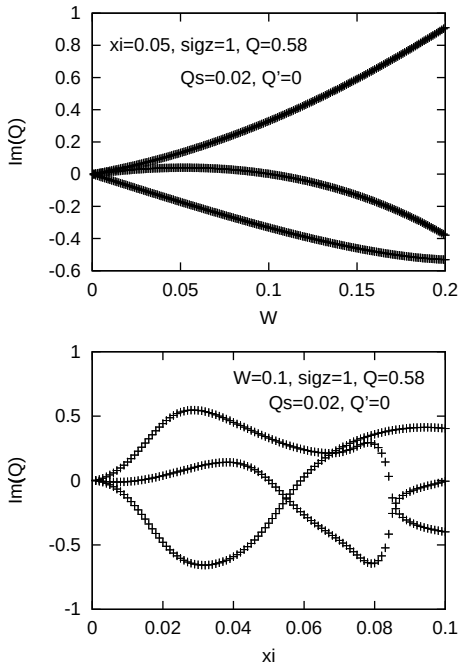

Figure 2: Dependence on the wake strength at $\xi = 0.05$ (upper) and the beam-beam parameter at W=0.1 (lower).

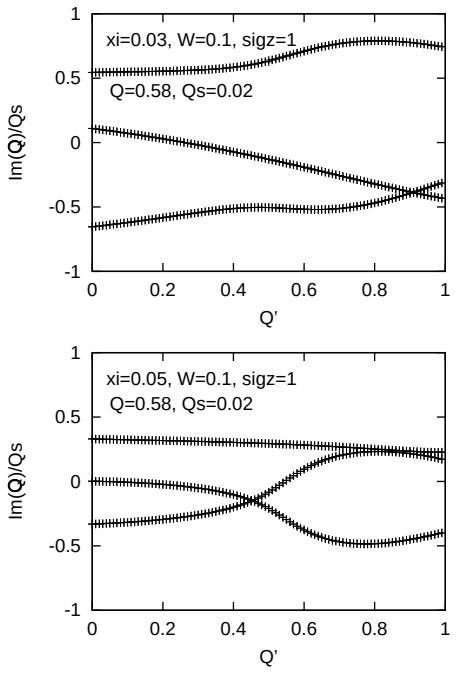

Figure 3: Chromaticity dependence. $\xi = 0.03$ (upper), $\xi = 0.05$ (lower).

We have imaginary part for $W > 0$. This means that horizontal effect should be taken care of.

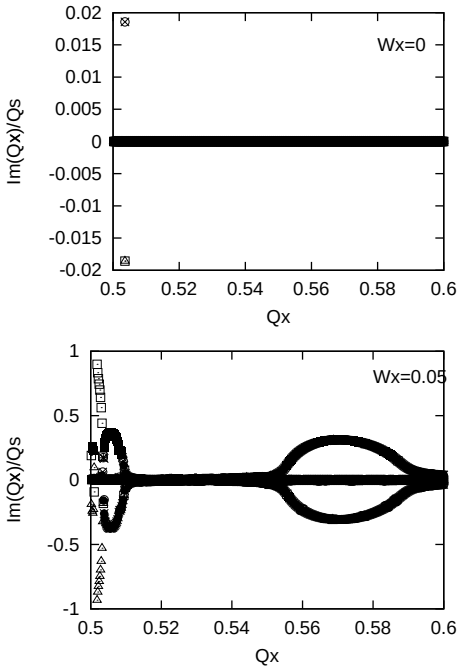

Figure 4: Dependence on horizontal tune. W=0 (upper), W=0.05 (lower). Note that the $W = 0$ case has an expanded vertical scale.

We assumed that the synchrotron tune was inverse of an integer. We extended the model to general synchrotron tune to avoid unphysical resonance behavior [5] by using a trick. We write down the transfer matrix for one synchrotron period

$$T_{syn} = T_{rev} \left(\frac{\sigma_z}{2}\right)^{\frac{1}{2\nu_s}} T_{rev} \left(-\frac{\sigma_z}{2}\right)^{\frac{1}{2\nu_s}} \qquad (25)$$

where ν_s is not an inverse of integer. We calculate the eigen value problem mathematically: i.e., in the eigen system, a noninteger power of matrix can be estimated. The collision points are assumed to be $\pm\sigma_z/2$ so that the transfer matrix is expressed by $1/2\nu_s$ power of the revolution matrices. We got results which are qualitatively consistent with the previous model.

We tried two-two particle model in which both beams are represented by two macro-particles. In this model we assumed the same sychrotron tunes for both beams. Similar results were obtained as for the one-two particle model. Further extensions are done by particle tracking simulation.

4 PARTICLE TRACKING SIMULATION USING MULTI-PARTICLE MODEL

We now proceed to a more realistic model. The beam-beam force is strongly nonlinear and the synchrotron tune is not an inverse of integer. The two beams have different

beam-beam parameters and different synchrotron and betatron tunes. Electron cloud is actully a crowd of electrons. The characteristic phase angle ϕ_e is larger than unity, and electrons are pinched by the beam force. We perform a particle tracking simulation to study the beam stability under these general conditions.

We represent the beams as a series of macro-particles (500$\sim$1,000) with a transverse Gaussian distribution of a fixed rms size [4]. For easy visualization, we use a multiple air-bag model for the longitudinal distribution, in which the micro-bunches are distributed on concentric circles in the longitudinal phase space, characterized by the position z and the relative momentum deviation $\Delta p/p$. The interaction starts from collision between the pair of micro-bunches of the two bunches with the largest value of $z_+ + z_-$, *i.e.*, the head of the two bunches, and then continues for other micro-particles pairs at progressively smaller $z_+ + z_-$ coordinates. The collision point of a pair is $s_\pm = \pm(z_+ - z_-)/2$ from viewpoints of positron and electron beams. The coordinate should be transferred into the collision point by a transformation $D(s_\pm)$ The macro-particles are transferred around the ring using a linear transport matrix and applying a chromaticity kick.

Electron cloud is represented by a large number of macro-electrons ($\sim$ $10,000$). The interaction between positron beam and electron cloud is evaluated by solving Eqs.(1) and (2) [4]. Electron cloud is put at a fixed position in the positron ring.

Figure 5 shows the variation of maximum vertical action $J_{y,max}$ of macro-particles with and without beam-beam interaction. The electron cloud density ($\rho_e = 2 \times 10^{11} m^{-3}$) used in the simulation is less than the threshold ($\rho_{e.th} = 5 \times 10^{11} m^{-3}$). We observe the fact that a remarkable difference with and without beam-beam interaction is due to combined effect of beam-beam and beam-electron cloud interactions. There was no growth for pure beam-beam interaction without electron cloud.

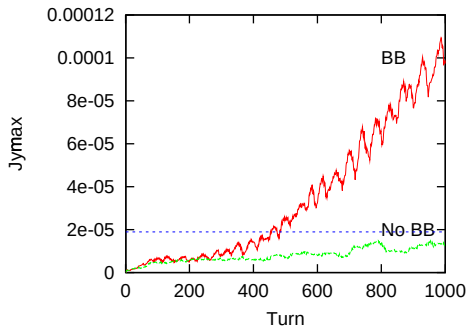

Figure 5: Combined effect of beam-beam and beam-electron cloud interactions. The two curves correspond to the variation of maximum $J_{y,max}$ of the macro-particles with and without beam-beam interaction.

Figure 6 shows the shape of the positron bunch projected onto the $y - z$ plane of the macro-particles positions after 400 and 800 turns. We can see a head-tail motion for the positron bunch experiencing both the beam-beam and the beam-electron cloud interaction.

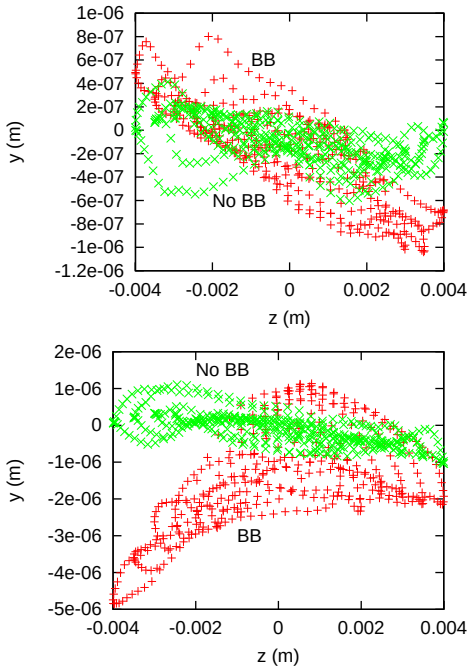

Figure 6: $y - z$ distribution of the positron bunch after 400 turns (upper) and 800 turns (lower). Different colors of the date points correspond to the bunch shapes with (red) and without (green) beam-beam interaction.

We next study effects of chromaticity and synchrotron tune spread. For a regular head-tail instability, it is well-known that chromaticity and synchrotron tune spread [6] affect its behavior. Figure 7 shows the dependence on chromaticity and synchrotron tune spread in our simulation. For the inclusion of tune spread effect, macro-particles are assumed to have a Gaussian distribution in the longitudinal phase space. These facts indicate that the chromaticity or synchrotron tune spread work to suppress the combined instability. However these effects are limited. For example, these parameters do not work well at a larger beam-beam parameter.

5 STRONG-STRONG BEAM-BEAM SIMULATION INCLUDING WAKE FIELD (PRELIMINARY)

The previous simulation is not sufficient for taking into account of nonlinearity of the beam-beam interaction, because betatron phase space location for a given syncrotron phase space location of a macro-particle is unique. Actually since there are many particles with various betatron coordinates in a region of synchrotron phase space, the beam-beam force may smear the betatron motion. To estimate the nonlinearity correctly, a strong-strong beam-beam

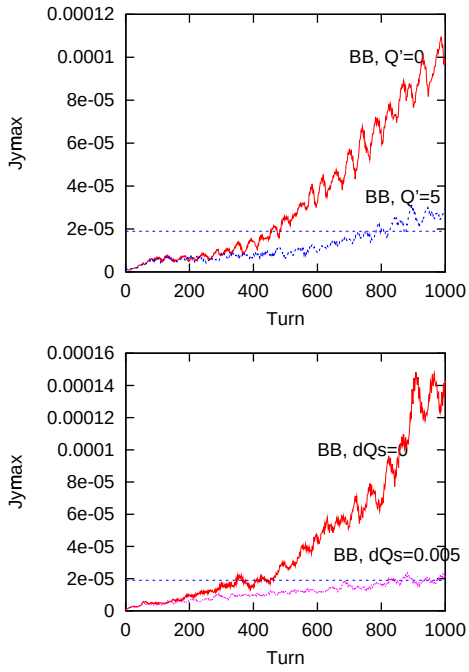

Figure 7: Dependence on chromaticity and synchrotron tune spread. Upper picture depicts evolution of J_y for $Q' = 5$ and $Q' = 0$, and lower picture depicts those for $\Delta\nu_s = 0$ and $\Delta\nu_s = 0.005$.

simulation, which treats interactions between many macro-particles, is required. Since it is complex to perform the strong-strong simulation for the both the beam-beam and beam-electron cloud effects, the beam-electron cloud interaction is approximated by an external wake field here [7]. We have already studied the beam-beam effect including wake field in two dimensional model [9], with the result that there was no remarkable effect. We now study three dimensional beam-beam system. Three dimensional beam-beam simulation is essential to study the present problem. However the three dimensional beam-beam simulation has a problem itself. The beam is divided into longitudinal slices, and slice by slice of collisions is calculated. To get a reliable result in the simulation, many longitudinal slices ($20 \sim 30$) were required depending on bunch length and beam-beam parameters. Since the calculation time scales quadratically with the number of slices, very long CPU time is required. We need to study how to integrate the three dimensional beam-beam interaction. Here a soft Gaussian approximation is used for simplification of the calculation.

A bunch is divided into N_{sl} slices which are denoted by $i = 1, N_{sl}$. We consider the collision between i-th positron slice and j-th electron slice. Beam envelope matrices for each slice are $R_{i+}(s^*)$ and $R_{j-}(s^*)$ at the design interaction point (s^*).

We propose a calculation algorithm. The algorithm has been used in weak-strong simulation [8]. We treat the collision of the two slices as collisions of positrons denoted by $a = 1, N_{i+}$ in i-th slice and j-th slice including N_{j-} electrons with an envelope R_{j-}. The role of positron bunch is exchanged for calculation of electron motion. The collision point of a-th positron and j-th electron slice is expressed by

$$s_{a+,j-} = \frac{z_{a+} - z_{j-}}{2}. \tag{26}$$

The a-th positron and j-th electron slice are transferred to the collision point $s_{a+,j-}$ according to

$$\begin{aligned} \boldsymbol{x}(s^* + s_{a+,j-}) &= D(s_{a+,j-})\boldsymbol{x}(s^*) \\ R_{j-}(s^* - s_{a+,j-}) &= D_l^{-1}(s_{a+,j-})R(s^*)D_l(s_{a+,j-}). \end{aligned} \tag{27}$$

D, which includes a dynamical variable z_{a+} of the a-th positron, is a nonlinear transformation. We take only linear part D_l for the transformation of R, while take nonlinear transformation D for $\boldsymbol{x}$. After the transformation, we calculate beam-beam interaction of the particle $\boldsymbol{x}_+$ for Gaussian beam represented by R_{j-}. We have to note that R_{j-} includes the dynamical variable z_{a+}.

This algorithm was essential to reduce the number of slices. Figure 8 shows the luminosity variation for new and old methods. The luminosity for the old method is extremely low. Increasing the number of slice for the old method, the luminosity is recovered near the level of the new method [11]. The slice number 5 is enough for the new method, while the old method requires 20-30 slices. The algorithm should be implemented in strong-strong beam-beam codes based on the Particle-In-Cell method [9, 10, 11, 12]. More details and study results will be presented elsewhere.

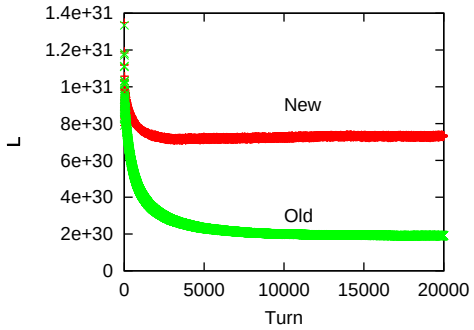

Figure 8: Luminosity variation for each turn. Bunches are divided into 5 slices. Luminosity calculated by the particle-slice algorithm is denoted by "New", while that by slice-slice algorithm is by "Old".

If all particles in the slices collide at a point,

$$s_{i+,j-} = \frac{z_{i+} - z_{j-}}{2}, \tag{28}$$

wrong results would be obtained yielding extremely low luminosity for a high current and long bunch length [11, 12].

We show very preliminary results of the 3-D soft Gaussian strong-strong beam-beam simulation including an external wake field.

Figure 9 shows the evolution of beam amplitudes, $\langle x_p \rangle$, $\langle y_p \rangle$, $\langle x_e \rangle$ and $\langle y_e \rangle$. We assume horizontal and vertical wake field, $W_x = 10^8 z[m^{-2}]$ and $W_y = 2 \times 10^8 z[m^{-2}]$. These strengths exceed a threshold of the vertical head-tail instability as is shown in the upper right picture. The vertical instability disappears when beam-beam interaction is included: beam-beam force suppresses the vertical head-tail instability. We found an enhancement of horizontal instability due to the beam-beam force as shown in the lower left picture. These results were unexpected from the linear theory and Gaussian simulation. We calculated the same model for sinusoidal wake fields $W_x = 2\times 10^6 \sin(213z)[m^{-2}]$ and $W_y = 1\times 10^7 \sin(570z)[m^{-2}]$ [7]. The results were similar to the Figure 9.

These behaviors are different from the linear theory and the Gaussian tracking simulation. We tried linear force for beam-beam interactions. We reduced the vertical wake field $W_y = 1.5\times 10^8 z[m^{-2}]$. There was no head-tail instability in both planes without beam-beam interaction. Figure 10 shows the evolution of beam amplitudes (upper two pictures), $y - z$ correlation (lower left) and vertical beam size (lower right). We found enhancement of the vertical instability due to the beam-beam interaction, but no effect for horizontal instability. These results are consistent with the linear theory and Gaussian simulation qualitatively.

These results should be studied further.

6 CONCLUSION

We studied combined phenomena of the beam-beam and beam-electron cloud effects using linear theory and a simulation with Gaussian approximation. In the linear theory, one-two particle model was used to describe the electron and positron beams. The electron cloud effect was approximated by a constant wake field. The beam-beam system without electron cloud effect was unstable at particular tune regions related to a synchro-beta resonance. while the combined system was always unstable regardless of the tune. The simulation with Gaussian approximation was performed to study the phenomena in general conditions. Below both thresholds of beam-beam and beam-cloud instabilities, an instability occurred due to thier combined effect in the simulation. We studied effects for the chromaticity and synchrotron tune spread. The combined phenomena may be analogous in its charercteristics to the regular head-tail effect.

We studied the phenomena using strong-strong beam-beam simulation. The results are preliminary, and should be studied further.

7 ACKNOWLEDGMENTS

This work is based on a collaboration of the authors at SLAC in the summer 2001. The authors thank E. Perevedentsev and A. Valishev for fruitful discussions. One of authors (K.O) thanks R. Ruth and Y. Cai for giving the chance of their collaboration. The author thanks F. Zimmermann for reading this manuscrit.

8 REFERENCES

[1] H. Fukuma, in this proceedings.

[2] E. A.Perevedentsev and A. A.Valishev, Phys. Rev. ST-AB, **4**, 024403 (2001); E. A. Perevedentsev, in Proc. of 1999 Part. Accel. Conf., New York, 1999, 1521 (1999); E. A. Perevedentsev, Proc. of Int. Workshop on Performance Improvement of Electron-Positron Collider Particle Factories, Tsukuba, 1999, KEK proceedings 99-24, 171 (1999).

[3] G. Rumolo and F. Zimmermann, CERN-SL-2001-0067. to be published in Proceedings of the Two-stream instability Workshop, Tsukuba (2001).

[4] K. Ohmi and F. Zimmermann, Phys. Rev. Lett., **85**, 3821 (2000).

[5] K. Oide, Private communications.

[6] P. Kernel, R. Nagaoka, J.-L. Revol, G. Besnier, EPAC 2000, Vienna (2000).

[7] K. Ohmi, F. Zimmermann, E. Perevedentsev, Phys. Rev. E **65**, 16502 (2002).

[8] K. Hirata, H. Moshammer and F. Ruggiero, Particle Accelerators, **40**, 205 (1993).

[9] K. Ohmi, Phys. Rev. E**62**, 7287 (2000).

[10] Y. Cai et. al.,Phys. Rev. ST-AB, **4**,011001 (2001).

[11] M. Tawada et. al., Proceedings of a Workshop on beam-beam effects in circular colliders, Fermilab, June 25-27, 2001, FERMILAB-Conf-01/390-T, 17 (2001).

[12] E. B.Anderson and J. T.Rogers, Proceedings of a Workshop on beam-beam effects in circular colliders, Fermilab, June 25-27, 2001, FERMILAB-Conf-01/390-T, 136 (2001).

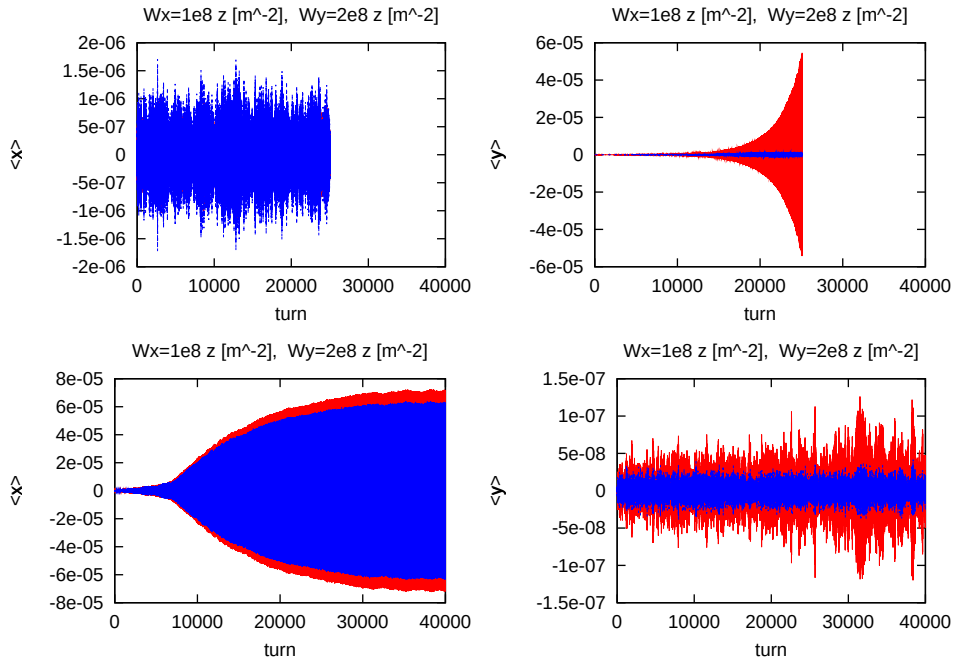

Figure 9: Evolution of beam amplitude for the strong-strong simulation including an external wake field. Red and blue curves correspond to amplitudes of positron and electron beams, respectively. Upper two pictures depict horizontal and vertical amplitudes without beam-beam interaction. Lower two pictures depict those with beam-beam interaction.

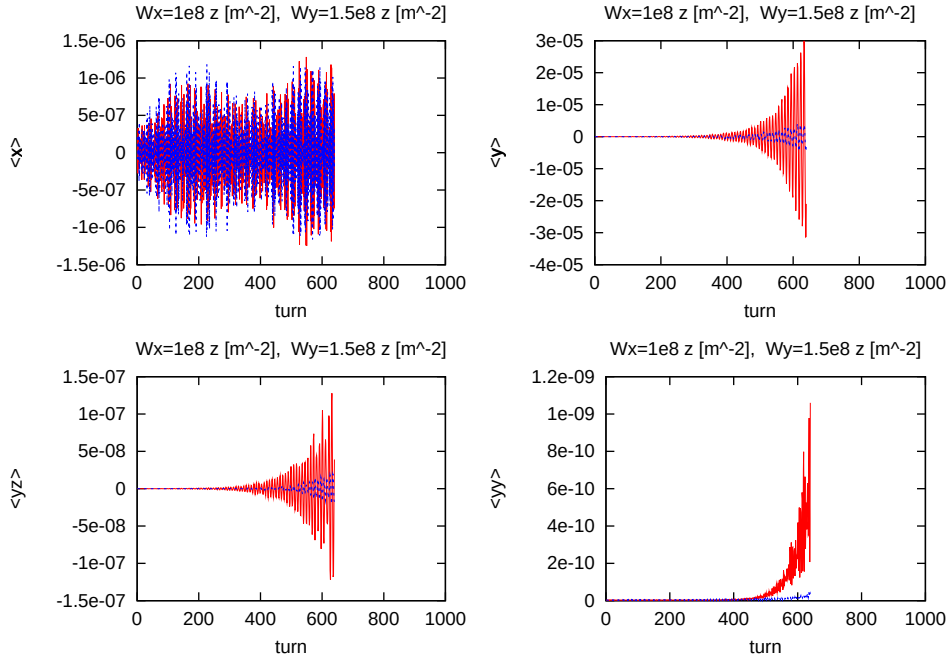

Figure 10: Evolution of beam amplitude for linear force including an external wake field. Red and blue curves correspond to amplitudes of positron and electron beams, respectively. Upper two pictures depict horizontal and vertical amplitudes with beam-beam interaction. Lower left picture depicts $y - z$ correlation $\langle yz \rangle$, and lower right depicts vertical beam size.